Blocking Wnt signaling by SFRP-like molecules inhibits in vivo cell proliferation and tumor growth in cells carrying active β-catenin.

Elise Lavergne, Ismaïl Hendaoui, Cédric Coulouarn, Catherine Ribault, Julie Leseur, Pierre-Antoine Eliat, Sihem Mebarki, Anne Corlu, Bruno Clément, Orlando Musso

Blocking Wnt signaling by SFRP-like molecules inhibits *in vivo* cell proliferation and tumor growth in cells carrying active β-catenin

Elise Lavergne, PhD[1,2], Ismaïl Hendaoui MSc[1,2], Cédric Coulouarn, PhD[1,2], Catherine Ribault BSc[1,2], Julie Leseur MD[1,2,3], Pierre-Antoine Eliat PhD[2,4], Sihem Mebarki MSc[1,2], Anne Corlu PhD[1,2], Bruno Clément PhD[1,2] and Orlando Musso MD, PhD[1,2].

[1] INSERM, UMR991, Liver Metabolisms and Cancer, F-35033 Rennes, France;

[2] Université de Rennes 1, F-35043 Rennes, France;

[3] Centre Régional de Lutte contre le Cancer, F-35042 Rennes, France;

[4] PRISM, IFR 140, Biogenouest®, F-35043 Rennes, France.

Running title: An SFRP-like *frizzled* motif blocks tumor growth

Financial support: Institut National de la Santé et de la Recherche Médicale, Institut National du Cancer, Agence Nationale de la Recherche (Emergence-BIO Program 2008), Université de Rennes 1, Région Bretagne.

Corresponding author: Orlando Musso, INSERM UMR991, Hôpital Pontchaillou, rue Henri Le Guilloux, 35033 RENNES Cedex, France. Phone: 33-2-99-54-74-08. Fax: 33-2-99-54-01-37. E-mail: orlando.musso@inserm.fr

Abbreviations: C18, collagen XVIII ; CM, conditioned medium ; CRC, colorectal carcinoma ; CRD, cystein-rich domain ; CRT, β-catenin-T-Cell factor Regulated Transcription ; DKK, *Dickkopf* ; DUF-959, domain of unknown function 959 ; FCS, fetal calf

serum ; FZC18, frizzled module of collagen XVIII ; GSEA, Gene Set Enrichment Analysis ; HCC, hepatocellular carcinoma ; HEK293, Human embryonic kidney 293; MMP-9, matrix metalloproteinase-9 ; MRI, magnetic resonance imaging ; NC, noncollagenous ; N-terminal, Nter ; SFRP, secreted frizzled related protein ; TCF, T-cell factor ; V2, variant 2 ; V3, variant 3 ; WIF-1, Wnt inhibitory factor-1 ; WT, wild-type.

Abstract

Constitutive activation of Wnt/β-catenin signaling in cancer results from mutations in pathway components, which frequently coexist with autocrine Wnt signaling or epigenetic silencing of extracellular Wnt antagonists. Among the extracellular Wnt inhibitors, the *secreted frizzled-related proteins* (SFRPs) are decoy receptors that contain soluble Wnt-binding frizzled domains. In addition to SFRPs, other endogenous molecules harboring frizzled motifs bind to and inhibit Wnt signaling. One of such molecules is V3Nter, a soluble SFRP-like frizzled polypeptide that binds to Wnt3a and inhibits Wnt signaling and expression of the β-catenin target genes cyclin D1 and *c-myc*. V3Nter is derived from the cell surface extracellular matrix component collagen XVIII. Here, we used HCT116 human colon cancer cells carrying the ΔS45 activating mutation in one of the alleles of β-catenin to show that V3Nter and SFRP-1 decrease baseline and Wnt3a-induced β-catenin stabilization. Consequently, V3Nter reduces the growth of human colorectal cancer xenografts by specifically controlling cell proliferation and cell cycle progression, without affecting angiogenesis or apoptosis, as shown by decreased [^{3}H] thymidine (*in vitro*) or BrdU (*in vivo*) incorporation, clonogenesis assays, cell cycle analysis and magnetic resonance imaging in living mice. Additionally, V3Nter switches off the β-catenin target gene expression signature *in vivo*. Moreover, experiments with β-catenin allele-targeted cells showed that the ΔS45 β-catenin allele hampers, but does not abrogate inhibition of Wnt signaling by SFRP-1 or by the SFRP-like frizzled domain. Finally, neither SFRP-1 nor V3Nter affect β-catenin signaling in SW480 cells carrying non functional APC. Thus, SFRP-1 and the SFRP-like molecule V3Nter can inhibit tumor growth of β-catenin-activated tumor cells *in vivo*.

Key words: frizzled, collagen XVIII, Wnt, β-catenin, colorectal cancer, secreted frizzled related proteins, tumor growth kinetics, tumor necrosis.

Introduction

The Wnt/β-catenin pathway is a major regulator of cell proliferation, migration, differentiation and metabolism, controlling tissue homeostasis and tumor progression (MacDonald *et al.*, 2009). In the majority of colorectal cancers (CRC), the coexistence of several mechanisms such as genetic defects in pathway components, autocrine Wnt signaling and epigenetic silencing of extracellular Wnt antagonists results in activation of Wnt/β-catenin signaling and provides a selective advantage to tumor cells (Polakis, 2007). Pathway activation involves interaction of Wnt ligands with cell surface Frizzled receptors and LRP5/6 co-receptors. This disrupts the *Adenomatous polyposis coli* (APC)-axin complex, thus halting proteasomal degradation of β-catenin, which is stabilized and interacts with T-cell factor (TCF) transcription factors, displacing repressors and recruiting activators of target gene expression.

The activity of the Wnt/β-catenin pathway can be antagonized by several families of secreted proteins. Interaction of Wnts ligands with the Frizzled receptors is enhanced by heparan sulfate glycosaminoglycans, controlling Wnt diffusion at the cell surface (Mikels and Nusse, 2006), or inhibited by several families of extracellular antagonists (Bovolenta *et al.*, 2008; Kawano and Kypta, 2003). Members of the *Dickkopf* (DKK) family antagonize canonical signaling by binding to LRP5/6, thus disrupting the Wnt-induced Frizzled-LRP5/6 complex (MacDonald *et al.*, 2009). Wnt inhibitory factor-1 (WIF-1) binds directly to Wnts, altering their ability to interact with the receptors. Members of the family of extracellular decoy receptors known as *secreted frizzled-related proteins* (SFRPs) possess a frizzled *cysteine-rich domain* (CRD) structurally similar to the extracellular Wnt-binding domain of the frizzled receptors. Frizzled CRDs contain 10 cysteines at conserved positions, which form a highly conserved 3D structure through a precise pattern of disulfide bridges. Frizzled CRDs

bind Wnts and form homodimers or heterodimers (Dann *et al.*, 2001). Thus, SFRPs can modulate Wnt signaling by sequestering Wnts through the CRD or by acting as dominant-negative inhibitors, forming inactive complexes with the frizzled receptors (Bovolenta *et al.*, 2008). In addition, engineered SFRP-like proteins such as the soluble CRD of the receptor Frizzled 8 potently inhibit autocrine Wnt signaling and tumor growth in mice carrying teratomas (DeAlmeida *et al.*, 2007).

It has been suggested that SFRPs may function as tumor suppressors in colorectal cancers because allelic loss or epigenetic inactivation of SFRP genes contributes to constitutive activation of the Wnt/β-catenin pathway (Caldwell *et al.*, 2004; Suzuki *et al.*, 2004). In this context, we and others have shown that restoring expression of SFRP-1 or SFRP-5 inhibits Wnt/β-catenin stabilization and induces *in vitro* cell death in human CRC cells (Quelard *et al.*, 2008; Suzuki *et al.*, 2004). In addition to SFRPs, other endogenous molecules carrying frizzled CRDs bind to and inhibit Wnt signaling. We recently showed that a frizzled CRD derived from cell surface collagen XVIII (C18) functions in an SFRP-like fashion, binding to Wnt3a and inhibiting Wnt/β-catenin signaling *in vitro* (Quelard *et al.*, 2008). C18 is expressed as three alternative tissue-specific variants, differing in their N-terminal (Nter) noncollagenous domains (Figure 1a), which are generated by two alternative promoters and mRNA splicing (Muragaki *et al.*, 1995; Rehn *et al.*, 1996). Variant 1 is a ubiquitous structural basement membrane component (Saarela *et al.*, 1998). Variant 2 (V2) is a plasma protein produced mainly in the liver (Musso *et al.*, 2001). Variant 3 (V3) is expressed at very low levels during *Xenopus* embryogenesis (Elamaa *et al.*, 2002), in human fetal (Elamaa *et al.*, 2003), in normal adult and tumor liver tissues (Quelard *et al.*, 2008) and is not detected in metastatic CRCs (Musso *et al.*, 2001). Proteolytic processing of V3 releases V3Nter, an aminoterminal glycoprotein containing a frizzled CRD, which locates at the cell

surface in cancer cells and matches the 3D structures of frizzled 8 and SFRP-3 CRDs (Quelard *et al.*, 2008).

These findings led us to explore the potential inhibitory effects of the frizzled module of C18 on tumor growth. We show here that V3Nter and SFRP-1 attenuate baseline and Wnt3a-induced β-catenin stabilization in HCT116 cells, reducing *in vitro* and *in vivo* tumor growth through slowed cell cycle progression. Moreover, V3Nter inhibits Wnt3a-induced β-catenin signaling in allele-targeted HCT116 cells carrying either wild-type or mutant β-catenin, confirming that V3Nter blocks tumor growth in the context of constitutively activated β-catenin.

Results

HCT116 colorectal cancer cells stably expressing V3Nter or SFRP-1 show low β-catenin levels

We produced HCT116 cell cultures stably expressing V3Nter (V3Nter-HCT116) or SFRP-1 (SFRP-1-HCT116) (Figures 1a and b). As negative controls, we prepared cells expressing either the homologous C18 polypeptide lacking the frizzled module (V2Nter-HCT116) or empty pCDNA3.1 vector (Vector-HCT116, Figures 1a and b). In HCT116 cells, transient expression of V3Nter, SFRP-1 or SFRP-5 induces cell death (Quelard *et al.*, 2008; Suzuki *et al.*, 2004). Consistently, attempts to obtain clones by limiting dilution were unsuccessful, suggesting a negative selection pressure, as shown for SFRP-1 in breast cancer cells (Bafico *et al.*, 2004). However, after seeding 3 cells/well, several antibiotic-resistant cell populations expressing the relevant epitopes (Supplementary Figure 1a) were expanded. By immunocytochemistry, they were composed of ~50% of cells expressing high levels of V3Nter or SFRP-1 and low β-catenin levels, and ~50% of cells showing low V3Nter or SFRP-1 content and high β-catenin levels (Figure 1c). In V3Nter (–) cells neighboring V3Nter (+) foci, β-catenin was restricted to cell membranes and particularly to cell contacts (Figure 1c, close-up), suggesting paracrine inhibition of Wnt/β-catenin signaling. Controls, *i.e.,* Vector- and V2Nter-HCT116 cells, showed widespread high β-catenin levels (Figure 1c). These features were stably maintained at least throughout 15 passages.

Consistently with our recent report using transient expression experiments (Quelard *et al.*, 2008), β-catenin-T-cell factor-regulated transcription (CRT) and cyclin D1 promoter activity were significantly decreased in HCT116 cells stably expressing V3Nter or SFRP-1, in contrast with cells expressing V2Nter or empty vector (Supplementary Figures 1b and c).

Similar effects on CRT were obtained with two different stable V3Nter cell batches (Supplementary Figure 1d).

Paracrine inhibtion of Wnt3a-induced β-catenin stabilization in HCT116 cells

V3Nter attenuated CRT in a dose-response assay to soluble Wnt3a (Figure 2a). By contrast, V2Nter enhanced CRT in this context (Figure 2a). Indeed, heparan sulfates attached to the 47-aa stretch common to the three C18 variants (Figure 1b) may locally increase Wnt concentration and thus CRT, as shown for C18 (Quelard *et al.*, 2008) and for other heparan sulfate proteoglycans (Mikels and Nusse, 2006). Accordingly, the slope of the Wnt3a dose-response curve for V2Nter-HCT116 cells was steeper than that of the other cells, including Vector-HCT116 cells. By contrast, V3Nter-HCT116 cells reached the maximal CRT under a 25% dilution of Wnt3a conditioned medium, further increases in Wnt3a concentration having no effect on CRT (Figure 2a). Immunoblot showed that basal and Wnt3a-induced levels of total β-catenin were lower in V3Nter- and SFRP-1-HCT116 cells than in Vector- or V2Nter-HCT116 cells (Figure 2b). These findings suggested that cell surface V3Nter could decrease β-catenin stabilization and transcriptional activity in response to soluble Wnt3a. Although soluble V3Nter and the FZC18 domain are detected in the conditioned medium at low levels, the bulk of the secreted proteins remain as cell surface forms (Quelard *et al.*, 2008). Therefore, FZC18-expressing cells might impact on the microenvironment of adjacent cells, thereby modulating their response to Wnt stimuli. To check this hypothesis, we co-cultured HEK293 cells stably expressing the frizzled domain of C18 (FZC18-HEK cells) with parental HCT116 cells expressing the CRT reporters. Co-cultures were established at different ratios of FZC18 (+) cells to a constant number of HCT116 reporter cells in the presence of 50% Wnt3a conditioned medium. Thus, the CRT response of HCT116 cells to soluble Wnt3a was

inversely proportional to the number of FZC18 (+) cells (Figure 2c). These findings confirm that V3Nter exerts its biological effects in the extracellular space.

V3Nter and SFRP-1 do not affect CRT in cells carrying non functional APC

Although V3Nter could inhibit baseline and Wnt3a-induced β-catenin stabilization in HCT116 cells carrying mutated β-catenin in one of the alleles, it was unable to modify CRT in the APC-mutated colorectal cancer cell line SW480 (Supplementary Figure 2a). As described (Morin *et al.*, 1997), CRT was dramatically reduced by expression of wild-type APC in SW480 cells. Since APC is required for β-catenin degradation (Yang *et al.*, 2006), these findings suggest that the effects of V3Nter are specific to the β-catenin pathway. Similarly, V3Nter did not induce significant effects on basal level CRT in cell lines carrying wild-type β-catenin such as human liver cancer Huh-7 and human cervical cancer HeLa cells. By contrast, both cell lines showed the expected CRT response to soluble Wnt3a, which was efficiently inhibited by V3Nter (Supplementary Figure 2b).

V3Nter and SFRP-1 inhibit Wnt signaling in cancer cells expressing either wild-type or mutant β-catenin

Extracellular Wnts provide a selective growth advantage to cancer cells containing heterozygous β-catenin mutations. This notion led us to ask whether this response relied solely on the wild-type β-catenin allele. Using HCT116 cell clones carrying either mutant ($CTNNB1^{-/\Delta S45}$) or wild-type ($CTNNB1^{WT/-}$) β-catenin (Chan *et al.*, 2002), we show that V3Nter and SFRP-1 expression decreased basal CRT by 50% and 30%, respectively, both in parental HCT116 cells and in the clone carrying only mutant β-catenin (Figure 3a). As previously described (Chan *et al.*, 2002), cells carrying only the wild-type allele showed no measurable CRT (Figure 3a). V3Nter inhibited Wnt3a-induced β-catenin signaling in allele-

targeted HCT116 cells carrying either wild-type or mutant β-catenin. As expected, inhibition was most efficient in cells carrying only the wild-type allele (Figures 3b and c). Similarly, SFRP-1 expression attenuated the CRT response to soluble Wnt3a in cells expressing either wild-type or mutant β-catenin (Supplementary Figure 2c). Negative controls confirmed the specificity of these findings (Supplementary Figure 2d). Taken together, these data show that expression of V3Nter inhibits soluble Wnt3a-induced β-catenin signaling in parental HCT116 cells (ΔS45/WT β-catenin), as well as in allele-targeted cells carrying either wild-type or mutant β-catenin. Inhibition is, however, most efficient in cells carrying only the wild-type allele, suggesting that, in parental HCT116 cells, the decrease in Wnt signaling results from the additive effects on both alleles of β-catenin. Consistently, in human CRC cells, phosphorylation of β-catenin at S45 seems not required for subsequent phosphorylation at residues S33, S37, or T41, in contrast to the prevailing models in normal cells (Wang *et al.*, 2003). However, S33 and S37 are essential for interaction with β-TrCP and subsequent β-catenin ubiquitination and degradation (Hart *et al.*, 1999). Therefore, as expected, in HEK293T cells transiently expressing S37A β-catenin or a dominant negative form of β-catenin lacking the S33, S37, T41 and S45 residues (Δ29-48 β-catenin), neither V3Nter nor SFRP-1 could inhibit CRT (not shown). Further experiments using FZC18 or SFRP-5 confirmed these findings (not shown).

V3Nter or SFRP-1 cDNAs inhibited the CRT increase induced by transiently expressed wild-type, S33Y or S37A β-catenins in Huh-7 human liver cancer cells carrying endogenous wild-type β-catenin (Figure 3d and Supplementary Figure 2e), suggesting that, in tumor cells, V3Nter and SFRP-1 may destabilize β-catenin through GSK3β and β-TrCP-independent pathways.

V3Nter reduces tumor cell proliferation in vitro through slowed cell cycle progression

Time course of [^{3}H] thymidine incorporation into newly synthesized DNA in response to serum stimulation showed a two-fold decrease in DNA synthesis in V3Nter- and in SFRP-1-HCT116 cells (Figure 4a). A different batch of V3Nter cells confirmed these data (Supplementary Figure 3a). These findings were further confirmed by analysis of mitochondrial succinate deshydrogenase activity (MTT assay) in a 96h time-course. In addition, this test showed no differences in cell survival 24h after plating (Supplementary Figure 3b). Consistently, a low apoptotic rate over a 72h time course was observed in HCT116 cells stably expressing V3Nter, SFRP-1 or V2Nter, as assessed by quantification of the subG1 population of cells by flow cytometry (Supplementary Figure 3c). Cell cycle analysis indicated that expression of V3Nter and SFRP-1 resulted in accumulation of cells in G0/G1 phase and a decrease in S-phase cells (Figure 4b).

Clonogenesis assays showed no difference in colony number between V3Nter or SFRP-1 and Vector HCT116 cells (Figure 4c, Supplementary Figure 4a), but V2Nter plates contained ~20% more colonies than Vector or V3Nter plates (Supplementary Figure 4a). This finding is consistent with the enhanced CRT in V2Nter cells shown above (Figure 2c) and with the 20% increase in clonogenesis that we previously showed in HCT116 cells expressing V2Nter (Quelard *et al.*, 2008). Interestingly, V3Nter-HCT116 cells showed reduced colony size with respect to Vector- and V2Nter-HCT116 cells (Figures 4c and d, Supplementary Figure 4b). Small colonies (1 to 1.5 mm in diameter) represented 65% of V3Nter- and 35% of SFRP-1-HCT116 colonies, but only 25% of Vector-HCT116 ones. Conversely, large colonies (3 to 4 mm in diameter) represented 30% of Vector- and 2% V3Nter- or 10% of SFRP-1-HCT116 ones. In V3Nter-HCT116 plates, small colonies arose more frequently than in V2Nter-HCT116 plates. Together with the above observations, *i.e.*, reduced cyclin D1 promoter activity and reduced DNA synthesis, but good cell viability; these findings suggest an inhibition on tumor cell proliferation rather than an effect on plating efficiency or viability.

A similar profile was described in HCT116 cells after inhibition of cyclin D1 expression by a dominant-negative TCF (Tetsu and McCormick, 1999).

V3Nter inhibits in vivo tumor growth through decreased cell proliferation

Xenografts of V3Nter-HCT116 cells in nude mice showed that V3Nter delayed tumor onset. More than 90% of the mice injected with Vector-HCT116 cells developed a solid tumor at day 13 whereas only 60% of the V3Nter-HCT116 cell-injected mice had a tumor on day 25 (Figure 5a). In addition, growth of V3Nter expressing tumors was significantly reduced. On day 22, the mean volume of these tumors was 7 folds smaller than that of the Vector-HCT116 tumors (Figures 5b and c, Supplementary Figure 5a). Two batches of V3Nter-HCT116 cells showed a similar growth pattern (Supplementary Figure 5b). SFRP-1 delayed tumor onset to a lesser extent. Indeed, 70% of the SFRP-1-HCT116 cell injected mice had a tumor on day 17, and 100% on day 25. On day 22, SFRP-1 reduced tumor growth by 2.2 fold, with respect to empty-vector expressing HCT116 cells. Tumor onset and growth of V2Nter- and Vector-HCT116 cells were not significantly different (Figures 5a-c, Supplementary Figure 5a). Throughout the experiment, V3Nter-HCT116 tumors expressed V3Nter, as shown by immunostaining at day 20 post subcutaneous injection (Supplementary Figure 6a).

Magnetic Resonance Imaging (MRI) in representative living mice revealed that the rapid growth curve of Vector-HCT116 tumors was associated with important hemorrhagic necrosis, which was not observed in V3Nter-HCT116 tumors (Figure 5d). T2-weighted signal showed large necrohemorrhagic foci in Vector- (day 14) but a very small focus in V3Nter- (day 18) HCT116 tumors (Figure 5d), which was confirmed by anatomic pathology tumor analysis after sacrifice of mice (data not shown).

We assessed cell proliferation, microvessel density and apoptosis *in situ* in V3Nter-HCT116 tumors by immunostaining with anti-BrdU, anti-CD31 or by the TUNEL assay.

Because *in vivo* labeling of S-phase cells with BrdU is influenced by tissue perfusion (Kyle *et al.*, 2003), we intravenously administered carbocyanine as a marker of functional blood vessels and searched for S-phase cells at any point ≤ 200 μm from a carbocyanine positive vessel.

As the growth kinetics of V3Nter-HCT116 cell tumors was different from that of control groups (Figure 5c), resulting in dramatically different final tumor sizes, we analyzed tumors of similar sizes (Mean±SD, Vector=148±152; V3Nter=146±96 mm^3, n=5 per group), representative of small, growing-phase tumors from both groups. The number of BrdU-labeled cells was significantly reduced in V3Nter- with respect to Vector-HCT116 cell tumors (Figure 6). To confirm these data, we immunostained cryosections derived from 6 additional tumors (Vector- or V3Nter-HCT116 tumors) with Ki67, a marker expressed on all proliferating cells during late G1, S, M and G2 phases of the cell cycle (Supplementary Figures 6b and c). Consistently, the number of Ki67-positive cells was reduced in V3Nter-HCT116 tumors compared to control ones. TUNEL assay, assessing DNA fragmentation, revealed no significant differences between the number of apoptotic cells in control and V3Nter-expressing tumors (Figure 6). Similarly, we observed no variation in microvessel density between Vector- and V3Nter-expressing tumors (Figure 6).

Taken together, these findings indicate that V3Nter expression delays tumor growth, profoundly changing the growth kinetics of HCT116 CRC cells *in vivo*.

V3Nter expressing tumors exhibit a switched off Wnt/β-catenin gene expression signature.

To determine whether V3Nter affected the expression of Wnt/β-catenin target genes, we obtained genome-wide expression profiles of Vector and V3Nter tumors and tested their enrichment in Wnt signaling gene expression signatures using Gene Set Enrichment Analysis (GSEA). GSEA evaluates microarray data focusing on previously published gene sets sharing

common biological function (Subramanian *et al.*, 2005). Gene sets were derived from two independent and curated Wnt activation signatures: loss of APC *in vivo* in the mouse intestine (Sansom *et al.*, 2004) and expression of a constitutively active mutant β-catenin by mammary cells (Kenny *et al.*, 2005). GSEA demonstrated that Vector and V3Nter gene expression profiles were respectively enriched in up- and down-regulated Wnt/β-catenin targets (Figure 7a, $p<0.05$). Consistently, microarray analysis revealed that V3Nter significantly reduced the expression of the β-catenin targets *Survivin*, *EpCAM*, *MMP-9*, *c-myc* and *Wnt3* among other genes (Figure 7b).

Discussion

The development of extracellular Wnt inhibitors working in the context of β-catenin pathway mutations is a promising therapeutic strategy. Enhanced autocrine Wnt signaling (Bafico *et al.*, 2004) and epigenetic silencing of genes encoding endogenous extracellular Wnt inhibitors (Suzuki *et al.*, 2004) provide a positive selection advantage to cells carrying β-catenin pathway mutations (Barker and Clevers, 2006; MacDonald *et al.*, 2009; Polakis, 2007). In this setting, frizzled receptor activation and enhanced Wnt expression drive positive cancer cell selection (Dimitriadis *et al.*, 2001; Holcombe *et al.*, 2002; Smith *et al.*, 1999; Ueno *et al.*, 2008; Vider *et al.*, 1996). Consequently, extracellular Wnt inhibitors such as SFRPs (Taketo, 2004), WIF1 (Hu *et al.*, 2009) or anti-Wnt1 antibodies (He *et al.*, 2005) block tumor cell growth in cells carrying mutant β-catenin.

In this work, we show that expression of a collagen-derived *frizzled* domain inhibits Wnt3a-induced β-catenin stabilization in HCT116 cells. V3Nter (–) cells neighboring V3Nter (+) foci showed low cytoplasmic and nuclear β-catenin content, suggesting that V3Nter could impact on the cell microenvironment. This notion was supported by paracrine inhibition of Wnt3a-induced CRT in cocultures of FZC18-expressing normal cells with parental HCT116 cells, indicating that the *frizzled* domain of C18 can inhibit Wnt signaling in the extracellular space.

V3Nter was unable to affect CRT in SW480 cells, which cannot degrade β-catenin as they lack functional APC (Yang *et al.*, 2006). Similarly, neither V3Nter nor SFRP-1 affected CRT in cancer cell lines carrying wild-type β-catenin. These findings suggest that the effects of V3Nter are specific to the Wnt/β-catenin pathway.

A previous report showed that SFRP-1 had no effect on growth of HCT116 cells *in vivo* (Bafico *et al.*, 2004). In that work, the authors used allele-targeted HCT116 cells carrying only wild-type β-catenin that exhibited elevated basal-level CRT as well as higher response to

serum growth factors and tumor growth than parental cells (Sekine *et al.*, 2002). By contrast, the wild-type β-catenin clone used here showed no measurable CRT and the *in vivo* growth of parental, mutant and wild-type HCT116 cells were not significantly different (Chan *et al.*, 2002), which probably explain the contrasting results.

We show that ΔS5 β-catenin does not completely abrogate inhibition of Wnt signaling by SFRP-like frizzled domains. Indeed, in colon cancer cells, priming phosphorylation at S45 of β-catenin does not seem required for subsequent phosphorylation of upstream residues S33, S37 and T41 (Wang *et al.*, 2003). Therefore, in parental HCT116 cells, inhibition of Wnt signaling results from the additive effects on both wild-type and mutant β-catenin alleles. As serines 33 and 37 of β-catenin are essential for β-TrCP-dependant β-catenin degradation (Hart *et al.*, 1999), neither V3Nter nor SFRP-1 inhibited CRT in HEK293T cells expressing mutant S33 or S37 β-catenins, implying a GSK3β and β-TrCP-dependent pathway. By contrast, in human liver cancer cells expressing either S37A or S33Y β-catenins, SFRP-1 and V3Nter did inhibit CRT, suggesting a GSK3β and β-TrCP-independent pathway.

An increasing body of evidence (He *et al.*, 2005; Suzuki *et al.*, 2004; Wang *et al.*, 2003) indicates that the mechanism of β-catenin degradation may be different in cancer cells with respect to normal cells (Liu *et al.*, 2002), supporting the notion that β-TrCP-independent pathways could be alternatively involved. Indeed, the ubiquitination of β-catenin by different E3 ligases that can bypass β-catenin phosphorylation occurs in specific contexts. For example, β-catenin can be degraded by Jade-1 (Chitalia *et al.*, 2008), Siah-1 or other ubiquitin ligases (Dimitrova *et al.*). Therefore, although the major mechanism of regulation of β-catenin activity is phosphorylation, the Wnt pathway may use multiple ways to regulate the concentration of β-catenin (Salahshor and Woodgett, 2005; Tolwinski and Wieschaus, 2004).

By Gene Set Enrichment Analysis, V3Nter-expressing tumors presented a switched off Wnt/β-catenin gene expression signature, further confirming inhibition of Wnt/β-catenin

signaling and downstream gene expression. Among the switched off genes, MMP-9 is involved in local invasion and metastasis (Takeuchi *et al.*, 2004), being secreted by macrophages and tumor infiltrating lymphocytes, as well as by CRC cells (Ahmed *et al.*, 2003). Survivin and c-myc are key regulators of cell growth in most human cancers and unfavorable prognostic markers, inhibiting cell death induced by several anticancer agents (Albihn *et al.*, ; Mita *et al.*, 2008). The epithelial cell adhesion molecule EpCAM is involved in a positive regulatory loop of Wnt signaling (Munz *et al.*, 2009).

We present compelling *in vitro* and *in vivo* data showing that a collagen-derived frizzled domain specifically blocks tumor cell growth through decreased cell proliferation and slowed cell cycle progression. V3Nter had a major impact on the growth kinetics of tumors. Likewise, MRI in living mice revealed that V3Nter-expressing tumors had minimal tumor necrosis with respect to the massive central necrosis seen in control HCT116 tumors. Spontaneous tumor necrosis is a hallmark of CRC, resulting in ominous clinical complications (Treanor and Quirke, 2007). It is the consequence of an insufficient vascular support to cope with rapid cell proliferation in fast growing tumors (Ramanujan *et al.*, 2000). Since inhibition of Wnt signaling slowed tumor growth, it restored the appropriate ratio of vascular support to tumor burden, thereby dramatically reducing necrosis. In conclusion, we show that an SFRP-like frizzled domain inhibits tumor growth in colorectal cancers. Its potential to attenuate cell growth and to sensitize to apoptosis may contribute to the development of new combined and personalized therapies that take into account the status of downstream β-catenin pathway components.

Materials and methods

cDNAs

V2Nter, V3Nter and SFRP-1 cDNAs, the Super8•TOP and Super8•FOP Flash reporters, the Cyclin D1 promoter reporter D1Δ-944pXP2, wild-type β-catenin and the normalization Renilla luciferase vector pGL4.70[*hRluc*] were previously described (Quelard *et al.*, 2008). S37A and Δ29-48 β-catenins were kindly provided by Y. Yang (Topol *et al.*, 2003). Vectors pcDNA3-S33Y β-catenin ((Kolligs *et al.*, 1999); Addgene plasmid 19286) and pCMV-Neo-Bam APC ((Morin *et al.*, 1997); Addgene plasmid 16507) were provided by E. Fearon and K Kinzler, respectively.

Mice and Tumors

Female athymic nude (*nu/nu*) mice were obtained from Iffa Credo (Charles River, France), housed under specific pathogen-free conditions and used for experiments at 6 weeks of age. All animal experimental procedures were carried out using Institutional Animal Care–approved protocols. Mice received $3x10^6$ tumor cells by subcutaneous injection in both hind legs in 100 µl FCS-free medium. Tumor size was measured three times a week with a digital caliper, and tumor volume was estimated from the following formula: width x length x (width + length)/2. Mice were sacrificed when the tumor volume reached ~1200 mm^3 or as indicated. Tumors were excised, snap frozen in liquid-nitrogen-cooled isopentane and stored at -80°C.

The BrdU incorporation assay was performed as described (Kyle *et al.*, 2003). Briefly, 20 days after tumor injection, BrdU (Sigma) was administered intraperitoneally 2h before sacrifice as a 50 mg/mL solution in saline at 1500 mg/kg. As a marker of tissue perfusion, mice were intravenously administered ~75 µl 0.6 mg/mL carbocyanine (Invitrogen) in 75% DMSO solution 5 min before sacrifice.

Gene expression profiling and Gene Set Enrichment Analysis (GSEA)

After histological analysis and homogeneization of ~400 mm3 of representative tumor tissue, RNA was extracted from Vector (n=3 tumors from 3 inoculation points from 3 mice) and V3Nter (n=6 tumors from 6 inoculation points from 3 mice). V3Nter tumors excised from the same mice were pooled. Total RNA was isolated by the Guanidinium Thiocyanate/Cesium Chloride method followed by a second extraction of the CsCl pellet with the NucleoSpin RNA II kit (Macherey-Nagel). In vitro transcription and labeling of 150ng total RNA was carried out using an Agilent Low-Input QuickAmp Labeling kit (Agilent Technologies) in the presence of Cy3-CTP following the manufacturer's protocol. After purification using a RNeasy mini kit (Qiagen), cRNA yield and specific activity were determined using a NanoDrop Spectrophotometer (yield, 9.2±0.5 µg cRNA ; specific activity, 20.0±0.4 pmol Cy3/µg cRNA). Equal amount (1.65 µg) of Cy3-labeled cRNA was subjected to fragmentation followed by 18h hybridization onto Agilent human 4x44K v2 pangenomic microarrays, washing, and scanning according to the manufacturer's instructions (Agilent Technologies). Gene expression data were further processed using Feature Extraction (version 10.7) and GeneSpring (version 11.0) software (Agilent Technologies). Filtration of array data resulted in the selection of 17,902 non-flag positive and significant gene features. Inter-arrays normalization was performed by using the 75th percentile signal value. GSEA was performed by using the web-based tool developed at the Broad Institute (Subramanian *et al.*, 2005) as previously described (Coulouarn *et al.*, 2009). Specific Wnt signatures (Kenny *et al.*, 2005; Sansom *et al.*, 2004) were retrieved using the curated collection C2 of Molecular Signatures Database (MSigDB).

Cell culture, transfection, reporter assays, cell growth assays, immunological methods, image acquisition and analysis, *in vivo* magnetic resonance imaging and statistical analysis were performed using standard methods. A detailed description is given in the Supplemental Materials and Methods section.

Acknowledgments

We thank technical assistance from C. Rocher at the Small Animal Imaging Platform, A. Fautrel and P. Bellaud at the Core HistoPathology Platform, R. Le Guével at the ImpactCell Platform, D. Le Quilleuc and B. Turlin at the Center for Biological Ressources and the animal husbandry group. We are indebted to B. Vogelstein, S. Bayling and H Suzuki, R. Moon, R. Nusse, T. Pihlajaniemi, and J. Pouyssegur for generously providing cells, cDNAs or antibodies and to Christine Perret (Institut Cochin, Department Endocrinology, Metabolism and Cancer, Paris, France) for critical reading of the manuscript.

Potential conflicts of interest

The following authors are co-authors of a patent owned by INSERM (Institut National de la Santé et de la Recherche Médicale) on the therapeutic use of the *frizzled* module of collagen XVIII: E. Lavergne, I. Hendaoui, J. Leseur, B. Clément and O. Musso. C. Coulouarn, C Ribault, P-A Eliat, S. Mebarki and A. Corlu declare no potential conflict of interest.

References

Ahmed N, Oliva K, Wang Y, Quinn M, Rice G (2003). Proteomic profiling of proteins associated with urokinase plasminogen activator receptor in a colon cancer cell line using an antisense approach. *Proteomics* **3:** 288-98.

Albihn A, Johnsen JI, Henriksson MA MYC in oncogenesis and as a target for cancer therapies. *Adv Cancer Res* **107:** 163-224.

Bafico A, Liu G, Goldin L, Harris V, Aaronson SA (2004). An autocrine mechanism for constitutive Wnt pathway activation in human cancer cells. *Cancer Cell* **6:** 497-506.

Barker N, Clevers H (2006). Mining the Wnt pathway for cancer therapeutics. *Nat Rev Drug Discov* **5:** 997-1014.

Bovolenta P, Esteve P, Ruiz JM, Cisneros E, Lopez-Rios J (2008). Beyond Wnt inhibition: new functions of secreted Frizzled-related proteins in development and disease. *J Cell Sci* **121:** 737-46.

Caldwell GM, Jones C, Gensberg K, Jan S, Hardy RG, Byrd P *et al* (2004). The Wnt antagonist sFRP1 in colorectal tumorigenesis. *Cancer Res* **64:** 883-8.

Chan TA, Wang Z, Dang LH, Vogelstein B, Kinzler KW (2002). Targeted inactivation of CTNNB1 reveals unexpected effects of beta-catenin mutation. *Proc Natl Acad Sci U S A* **99:** 8265-70.

Chitalia VC, Foy RL, Bachschmid MM, Zeng L, Panchenko MV, Zhou MI *et al* (2008). Jade-1 inhibits Wnt signalling by ubiquitylating beta-catenin and mediates Wnt pathway inhibition by pVHL. *Nat Cell Biol* **10:** 1208-16.

Coulouarn C, Factor VM, Andersen JB, Durkin ME, Thorgeirsson SS (2009). Loss of miR-122 expression in liver cancer correlates with suppression of the hepatic phenotype and gain of metastatic properties. *Oncogene* **28:** 3526-36.

Dann CE, Hsieh JC, Rattner A, Sharma D, Nathans J, Leahy DJ (2001). Insights into Wnt binding and signalling from the structures of two Frizzled cysteine-rich domains. *Nature* **412:** 86-90.

de La Coste A, Romagnolo B, Billuart P, Renard CA, Buendia MA, Soubrane O *et al* (1998). Somatic mutations of the beta-catenin gene are frequent in mouse and human hepatocellular carcinomas. *Proc Natl Acad Sci U S A* **95:** 8847-51.

DeAlmeida VI, Miao L, Ernst JA, Koeppen H, Polakis P, Rubinfeld B (2007). The soluble wnt receptor Frizzled8CRD-hFc inhibits the growth of teratocarcinomas in vivo. *Cancer Res* **67:** 5371-9.

Dimitriadis A, Vincan E, Mohammed IM, Roczo N, Phillips WA, Baindur-Hudson S (2001). Expression of Wnt genes in human colon cancers. *Cancer Lett* **166:** 185-91.

Dimitrova YN, Li J, Lee YT, Rios-Esteves J, Friedman DB, Choi HJ *et al* Direct ubiquitination of beta-catenin by Siah-1 and regulation by the exchange factor TBL1. *J Biol Chem* **285:** 13507-16.

Elamaa H, Peterson J, Pihlajaniemi T, Destree O (2002). Cloning of three variants of type XVIII collagen and their expression patterns during Xenopus laevis development. *Mech Dev* **114:** 109-13.

Elamaa H, Snellman A, Rehn M, Autio-Harmainen H, Pihlajaniemi T (2003). Characterization of the human type XVIII collagen gene and proteolytic processing and tissue location of the variant containing a frizzled motif. *Matrix Biol* **22:** 427-42.

Hart M, Concordet JP, Lassot I, Albert I, del los Santos R, Durand H *et al* (1999). The F-box protein beta-TrCP associates with phosphorylated beta-catenin and regulates its activity in the cell. *Curr Biol* **9:** 207-10.

He B, Reguart N, You L, Mazieres J, Xu Z, Lee AY *et al* (2005). Blockade of Wnt-1 signaling induces apoptosis in human colorectal cancer cells containing downstream mutations. *Oncogene* **24:** 3054-8.

Holcombe RF, Marsh JL, Waterman ML, Lin F, Milovanovic T, Truong T (2002). Expression of Wnt ligands and Frizzled receptors in colonic mucosa and in colon carcinoma. *Mol Pathol* **55:** 220-6.

Hu J, Dong A, Fernandez-Ruiz V, Shan J, Kawa M, Martinez-Anso E *et al* (2009). Blockade of Wnt signaling inhibits angiogenesis and tumor growth in hepatocellular carcinoma. *Cancer Res* **69:** 6951-9.

Kawano Y, Kypta R (2003). Secreted antagonists of the Wnt signalling pathway. *J Cell Sci* **116:** 2627-34.

Kenny PA, Enver T, Ashworth A (2005). Receptor and secreted targets of Wnt-1/beta-catenin signalling in mouse mammary epithelial cells. *BMC Cancer* **5:** 3.

Kolligs FT, Hu G, Dang CV, Fearon ER (1999). Neoplastic transformation of RK3E by mutant beta-catenin requires deregulation of Tcf/Lef transcription but not activation of c-myc expression. *Mol Cell Biol* **19:** 5696-706.

Kyle AH, Huxham LA, Baker JH, Burston HE, Minchinton AI (2003). Tumor distribution of bromodeoxyuridine-labeled cells is strongly dose dependent. *Cancer Res* **63:** 5707-11.

Liu C, Li Y, Semenov M, Han C, Baeg GH, Tan Y *et al* (2002). Control of beta-catenin phosphorylation/degradation by a dual-kinase mechanism. *Cell* **108:** 837-47.

MacDonald BT, Tamai K, He X (2009). Wnt/beta-catenin signaling: components, mechanisms, and diseases. *Dev Cell* **17:** 9-26.

Mikels AJ, Nusse R (2006). Wnts as ligands: processing, secretion and reception. *Oncogene* **25:** 7461-8.

Mita AC, Mita MM, Nawrocki ST, Giles FJ (2008). Survivin: key regulator of mitosis and apoptosis and novel target for cancer therapeutics. *Clin Cancer Res* **14:** 5000-5.

Morin PJ, Sparks AB, Korinek V, Barker N, Clevers H, Vogelstein B *et al* (1997). Activation of beta-catenin-Tcf signaling in colon cancer by mutations in beta-catenin or APC. *Science* **275:** 1787-90.

Munz M, Baeuerle PA, Gires O (2009). The emerging role of EpCAM in cancer and stem cell signaling. *Cancer Res* **69:** 5627-9.

Muragaki Y, Timmons S, Griffith CM, Oh SP, Fadel B, Quertermous T *et al* (1995). Mouse Col18a1 is expressed in a tissue-specific manner as three alternative variants and is localized in basement membrane zones. *Proc Natl Acad Sci U S A* **92:** 8763-7.

Musso O, Theret N, Heljasvaara R, Rehn M, Turlin B, Campion JP *et al* (2001). Tumor hepatocytes and basement membrane-Producing cells specifically express two different forms of the endostatin precursor, collagen XVIII, in human liver cancers. *Hepatology* **33:** 868-76.

Polakis P (2007). The many ways of Wnt in cancer. *Curr Opin Genet Dev* **17:** 45-51.

Quelard D, Lavergne E, Hendaoui I, Elamaa H, Tiirola U, Heljasvaara R *et al* (2008). A cryptic frizzled module in cell surface collagen 18 inhibits Wnt/beta-catenin signaling. *PLoS ONE* **3:** e1878.

Ramanujan S, Koenig GC, Padera TP, Stoll BR, Jain RK (2000). Local imbalance of proangiogenic and antiangiogenic factors: a potential mechanism of focal necrosis and dormancy in tumors. *Cancer Res* **60:** 1442-8.

Rehn M, Hintikka E, Pihlajaniemi T (1996). Characterization of the mouse gene for the alpha 1 chain of type XVIII collagen (Col18a1) reveals that the three variant N-terminal polypeptide forms are transcribed from two widely separated promoters. *Genomics* **32:** 436-46.

Saarela J, Rehn M, Oikarinen A, Autio-Harmainen H, Pihlajaniemi T (1998). The short and long forms of type XVIII collagen show clear tissue specificities in their expression and location in basement membrane zones in humans. *Am J Pathol* **153:** 611-26.

Salahshor S, Woodgett JR (2005). The links between axin and carcinogenesis. *J Clin Pathol* **58:** 225-36.

Sansom OJ, Reed KR, Hayes AJ, Ireland H, Brinkmann H, Newton IP *et al* (2004). Loss of Apc in vivo immediately perturbs Wnt signaling, differentiation, and migration. *Genes Dev* **18:** 1385-90.

Sekine S, Shibata T, Sakamoto M, Hirohashi S (2002). Target disruption of the mutant beta-catenin gene in colon cancer cell line HCT116: preservation of its malignant phenotype. *Oncogene* **21:** 5906-11.

Smith K, Bui TD, Poulsom R, Kaklamanis L, Williams G, Harris AL (1999). Up-regulation of macrophage wnt gene expression in adenoma-carcinoma progression of human colorectal cancer. *Br J Cancer* **81:** 496-502.

Subramanian A, Tamayo P, Mootha VK, Mukherjee S, Ebert BL, Gillette MA *et al* (2005). Gene set enrichment analysis: a knowledge-based approach for interpreting genome-wide expression profiles. *Proc Natl Acad Sci U S A* **102:** 15545-50.

Suzuki H, Watkins DN, Jair KW, Schuebel KE, Markowitz SD, Chen WD *et al* (2004). Epigenetic inactivation of SFRP genes allows constitutive WNT signaling in colorectal cancer. *Nat Genet* **36:** 417-22.

Taketo MM (2004). Shutting down Wnt signal-activated cancer. *Nat Genet* **36:** 320-2.

Takeuchi T, Hisanaga M, Nagao M, Ikeda N, Fujii H, Koyama F *et al* (2004). The membrane-anchored matrix metalloproteinase (MMP) regulator RECK in combination with MMP-9 serves as an informative prognostic indicator for colorectal cancer. *Clin Cancer Res* **10:** 5572-9.

Tetsu O, McCormick F (1999). Beta-catenin regulates expression of cyclin D1 in colon carcinoma cells. *Nature* **398:** 422-6.

Tolwinski NS, Wieschaus E (2004). Rethinking WNT signaling. *Trends Genet* **20:** 177-81.

Topol L, Jiang X, Choi H, Garrett-Beal L, Carolan PJ, Yang Y (2003). Wnt-5a inhibits the canonical Wnt pathway by promoting GSK-3-independent beta-catenin degradation. *J Cell Biol* **162:** 899-908.

Treanor D, Quirke P (2007). Pathology of colorectal cancer. *Clin Oncol (R Coll Radiol)* **19:** 769-76.

Ueno K, Hiura M, Suehiro Y, Hazama S, Hirata H, Oka M *et al* (2008). Frizzled-7 as a potential therapeutic target in colorectal cancer. *Neoplasia* **10:** 697-705.

Vider BZ, Zimber A, Chastre E, Prevot S, Gespach C, Estlein D *et al* (1996). Evidence for the involvement of the Wnt 2 gene in human colorectal cancer. *Oncogene* **12:** 153-8.

Wang Z, Vogelstein B, Kinzler KW (2003). Phosphorylation of beta-catenin at S33, S37, or T41 can occur in the absence of phosphorylation at T45 in colon cancer cells. *Cancer Res* **63:** 5234-5.

Yang J, Zhang W, Evans PM, Chen X, He X, Liu C (2006). Adenomatous polyposis coli (APC) differentially regulates beta-catenin phosphorylation and ubiquitination in colon cancer cells. *J Biol Chem* **281:** 17751-7.

Figure legends

Figure 1. HCT116 colorectal cancer cells stably expressing a C18-derived *frizzled* module or SFRP-1 show low β-catenin levels. (**a**) Schematic structure of the three variants of full length C18 differing by their specific aminoterminal noncollagenous (Nter NC) domains. Both V2 and V3 contain the 192 aa Domain of Unknown Function-959 (DUF-959) at their N-termini. V3 has a 235 aa module containing a 117 aa frizzled cysteine-rich domain (CRD). The three variants share common C-terminal sequences, including the thrombospondin-1 (Tsp-1) module, heparan sulfate attachment sites (HS), a highly interrupted collagenous sequence, and the endostatin (ES) module. (**b**) V3Nter, SFRP-1 and V2Nter expression vectors. Thick horizontal lines indicate the antibodies used. Grey box, 47-aa stretch from the Tsp-1 module. V5, V5 tag. NTR, netrin module. (**c**) HCT116 cells stably expressing V3Nter or SFRP-1 show low β-catenin levels. Immunofluorescent detection of β-catenin in HCT116 cells stably expressing V3Nter, V2Nter or SFRP-1 *(top)*. Antibodies are indicated on the left. Anti-DUF-959 detects an epitope common to V2Nter and V3Nter. Cells expressing V3Nter or SFRP-1 show low β-catenin levels (*arrows*), but cells expressing low V3Nter or SFRP-1 levels show high β-catenin (*arrowheads*). Images were acquired by automatic tiling of adjacent fields at original magnification x200. Close-up shows that V3Nter-expressing cells contain low nuclear and cytoplasmic β-catenin levels.

Figure 2. V3Nter and SFRP-1 attenuate baseline and Wnt3a-induced β-catenin stabilization in HCT116 cells. Gene assays using the CRT reporter Super8•TOP Flash in HCT116 cells. (**a**) Relative CRT in the HCT116 cells. Twenty-four hours after transfection with the CRT reporter, cells were incubated with either control-CM (conditioned medium) or Wnt3a-CM at the indicated dilutions for 16h. *Below,* aliquots from Wnt3a-conditioned media were immunoblotted with anti-Wnt3a. (**b**) HCT116 cells stably transfected with the indicated

expression vectors (*top*) were incubated with 100% control-CM (–) or 50% Wnt3a-CM (+). Total protein extracts from these cells were analyzed by western blotting detecting anti-β-catenin. The same blot was probed with anti-GAPDH as a loading standard. (**c**) Relative CRT in parental HCT116 cells transfected with Super8•TOP or FOP Flash reporters and co-cultured with HEK293T cells stably expressing FZC18 or empty vector at different ratios, as indicated in the presence of 50% Wnt3a-CM. *Below,* total protein extracts from these cells were immunoblotted with anti-myc epitope tag detecting FZC18. The same blot was probed with anti-GAPDH as a loading standard.

Figure 3. **V3Nter inhibits Wnt signaling in cancer cells carrying either wild-type or mutant β-catenin.** (**a**) V3Nter and SFRP-1 attenuate CRT in parental HCT116 cells (CTNNB1$^{WT/\Delta S45}$) and in cells containing only mutant β-catenin. HCT116 cells lacking mutant β-catenin (CTNNB1$^{WT/-}$) have no measurable CRT. (**b**) V3Nter inhibits the CRT response to soluble Wnt3a in cells containing either wild-type or mutant β-catenin. After transient transfection with the indicated vectors, cells were challenged with Wnt3a-CM in a dose-response assay for 16h. Super8•TOP Flash data show mean±SD from three replications. Super8•FOP Flash data are shown in Figure S2d. The slopes of the dose-response curves indicate that V3Nter inhibits CRT most efficiently in cells containing only wild-type β-catenin. (**c**) Inhibition of β-catenin stabilization by V3Nter in response to soluble Wnt3a in CTNNB1$^{WT/-}$ and $^{-/\Delta S45}$ HCT116 cell clones. After transient transfection with the indicated vectors, cells were incubated with either 100% control-CM (–) or 100% Wnt3a-CM (+) for 16h and total protein was analyzed by immunoblot. Hsc-70 is a loading standard. (**d**) Relative CRT in Huh-7 human liver cancer cells (endogenous wild-type β-catenin (de La Coste *et al.*, 1998)) transiently transfected with the Super8•TOP Flash reporter and the indicated β-catenin

expression vectors. CRT is shown relative to cells expressing empty vector. Super8•FOP Flash data are shown in Figure S2e.

Figure 4. **V3Nter reduces *in vitro* tumor cell proliferation.** (**a** and **b**) Analysis of DNA synthesis and cell cycle distribution in HCT116 cells stably expressing the indicated vectors, shown as mean±SD from three replications. (**a**) [^{3}H] thymidine incorporation. Cell cycle synchronized cells were stimulated with 10% FCS in a 72h time course. At the indicated time points, cells were pulsed with [^{3}H] thymidine for 90 min, lyzed and [^{3}H] thymidine measured using a scintillation counter. (**b**) Cell cycle distribution. At the indicated time points after seeding, cells were stripped from dishes and analyzed by flow cytometry after propidium iodide staining. A total of 1 x 10^4 cells were analyzed in each triplicate. Asterisks indicate statistic significance of the differences between Vector's and other groups' means at 72h (Student *"t"* test, $p< 0.005$). (**c**) HCT116 cells stably transfected with the indicated expression vectors were seeded at low density and cultured for 14 days. After paraformaldehyde fixing and hematoxylin staining, colonies (seen as dark spots) were digitized using a video camera. (**d**) After printing photographs of colony-containing dishes, colonies were measured, assigned to size categories and blindly counted using a grid. Histograms represent distribution of cells in each category of colony size (mean±SD from three replications). V3Nter-HCT116 colonies are significantly smaller than Vector- or V2Nter-HCT116 colonies. Statistical analysis is shown in Supplementary Figure 4b.

Figure 5. V3Nter inhibits the growth of HCT116 tumor xenografts *in vivo.* Athymic nude mice received subcutaneous injections of HCT116 cells stably expressing the indicated vectors. (**a**) Six mice per group received cells in both hind legs. At each time point, the percentage of tumor-free mice is indicated. (**b**) Representative photographs of mice carrying

subcutaneous tumors 20 days after injection (*arrows*). (**c**) Analysis of tumor volume [width x length x (width + length)/2] in a 22-day time course. Statistical analysis is shown in Supplementary Figure 5a. (**d**) Representative T1- and T2-weighted resonance magnetic images of Vector- or V3Nter-HCT116 tumor xenografts. Vector-HCT116 tumor shows important necro-hemorrhagic foci in contrast to V3Nter-HCT116 tumor (*arrows*). "D" indicates day post subcutaneous injection. Images were acquired on living mice placed in a supine position using a 4.7 Tesla horizontal Biospec Imaging System.

Figure 6. V3Nter reduces tumor cell proliferation *in vivo*. Mice carrying Vector- or V3Nter-HCT116 tumors were pulsed by intraperitoneal injection of BrdU and intravenous injection of carbocyanine 120 and 5 min before sacrifice, respectively. (**a**) Cell proliferation, angiogenesis and apoptosis were assessed in tumor cryosections by immunostaining with anti-BrdU, anti-CD31 or by the TUNEL assay, respectively. BrdU (+) S-phase cells (*brown*) are shown relative to non S-phase cells (hematoxylin, *light blue*) and to functional blood vessels (carbocyanine, *green*). Fluorescent images of carbocyanine-labeled vessels were acquired from fresh cryosections and overlaid on subsequent bright-field images after immunostaining with anti-BrdU and counterstaining with hematoxylin. Apoptotic TUNEL-labeled cells (*green, arrows*) or CD31 (+) blood vessels (*red, arrows*) are shown relative to nuclear staining with the fluorescent dye DAPI (*blue*). (**b**) To quantify S-phase cells, images were acquired from whole mount tissue sections in well perfused carbocyanine (+) areas, using a Micro Imager M1 microscope (Zeiss) and Zeiss AxioVision Software. BrdU (+) cells were counted with Image J (NIH). TUNEL and CD31 signals were quantified with Simple PCI 6.1.2. Bar graphs show mean±SD from five tumors. NS, non significant; *, $p<0.05$ (Mann-Whitney U-test).

Figure 7. V3Nter expressing tumors exhibit a switched off Wnt/β-catenin gene expression signature. Tumors derived from Vector- and V3Nter-overexpressing HCT116 cells were profiled using pangenomic microarrays. (**a**) Gene Set Enrichment Analysis (GSEA) was performed using two independent and curated Wnt activation signatures: *upper panels,* gene expression signature from cells expressing a constitutively active β-catenin mutant; *lower panels, in vivo* APC loss gene signature. Top portion of the plots displays the running Enrichment Score for the gene signatures along the ranked gene expression dataset (left side, V3Nter; right side, Vector). Bar codes indicate the position of members of the specific gene signatures in the ranked-ordered gene dataset. Vector and V3Nter gene expression profiles were respectively enriched in up- and down-regulated Wnt/β-catenin targets ($p<0.05$). (**b**) Relative expression of well-known Wnt/β-catenin target genes in Vector- and V3Nter-overexpressing HCT116 cells. V3Nter significantly reduced the expression of *Survivin*, *EpCAM*, *MMP-9*, *c-myc* and *Wnt3* (two-tailed Student's t-test: * $p<.05$, ** $p<.01$, *** $p<.001$). Data are expressed as mean±SD (n=3).

Figure 1 - Lavergne *et al.*

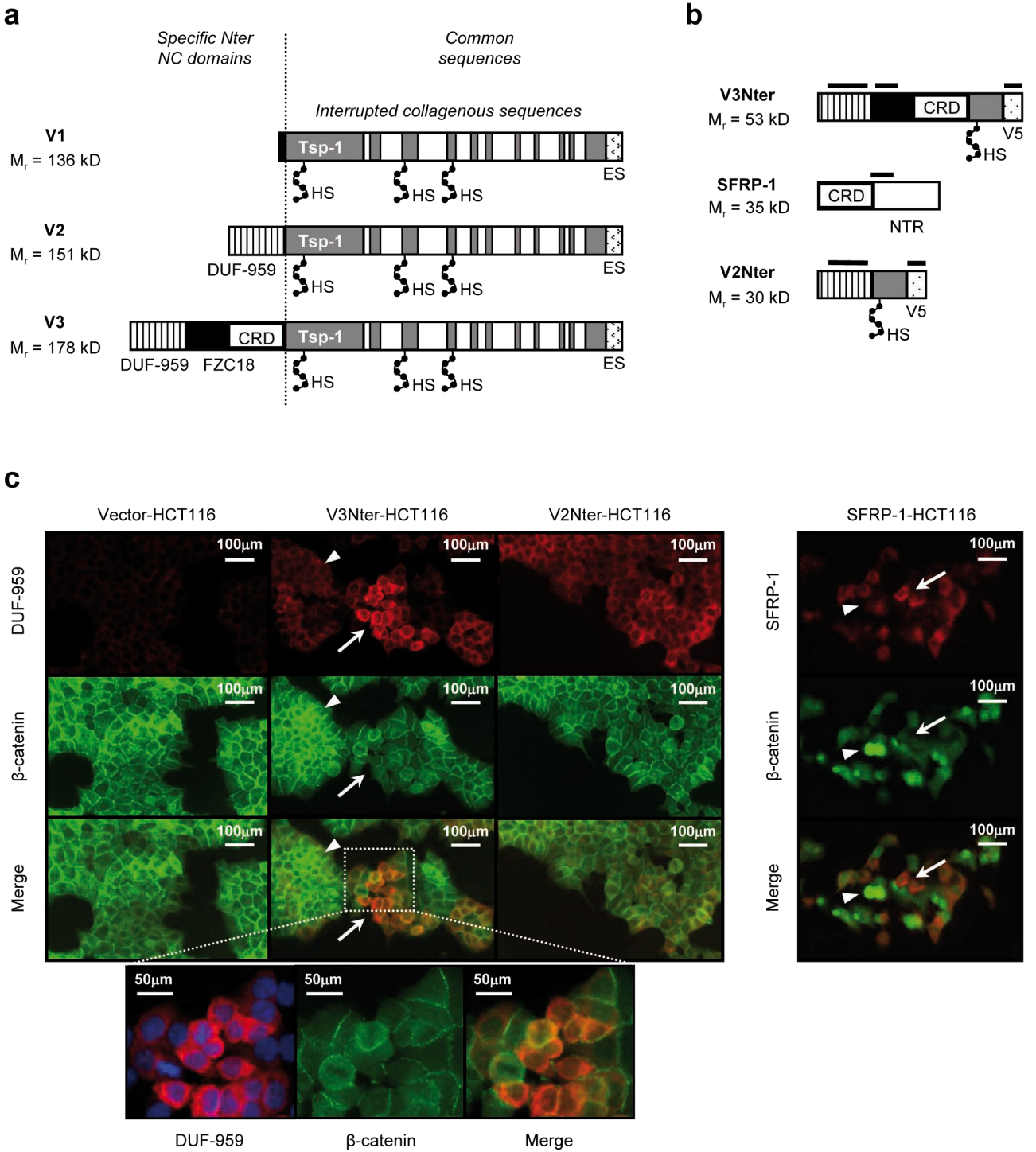

Figure 2 - Lavergne *et al.*

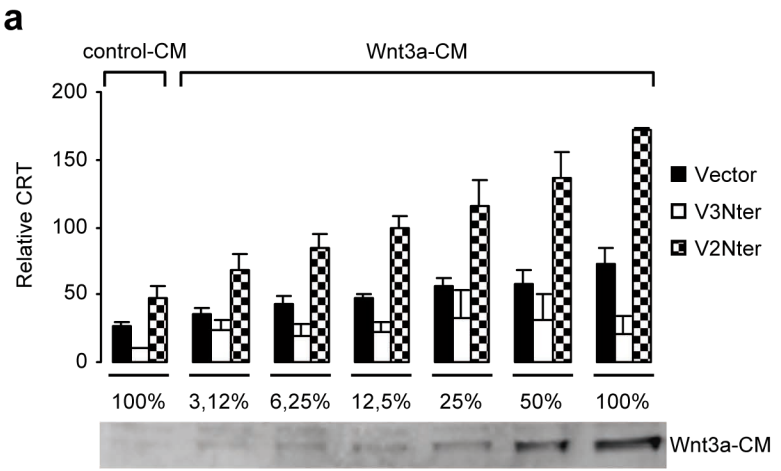

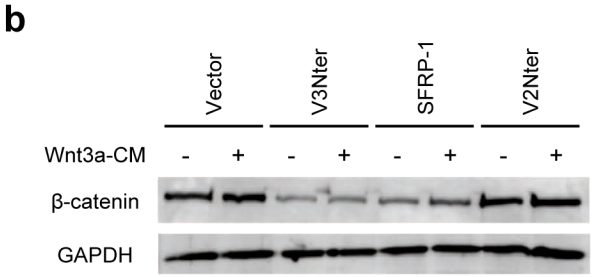

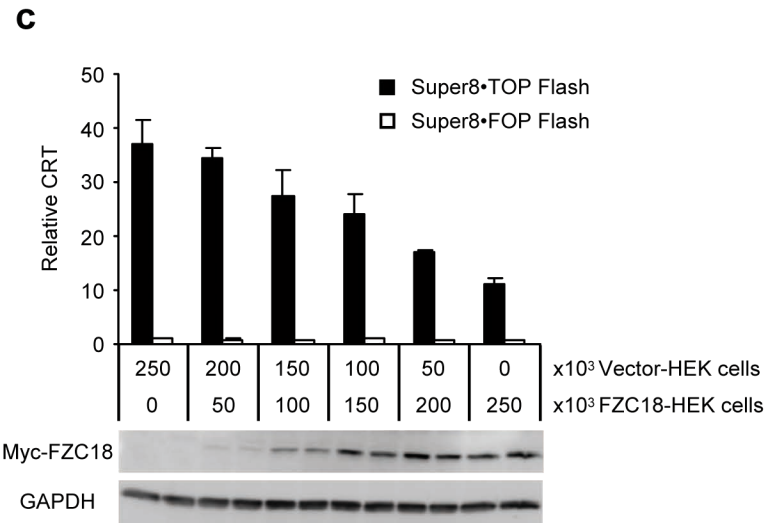

Figure 3 - Lavergne *et al.*

a

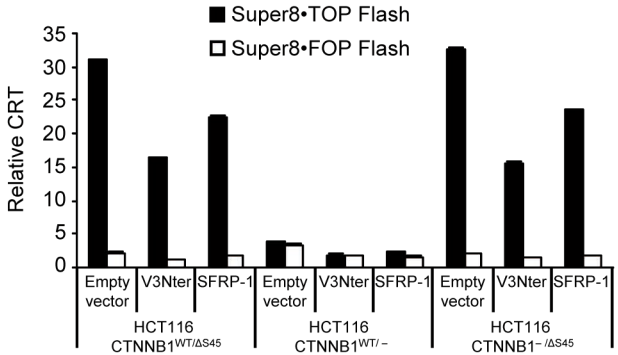

b

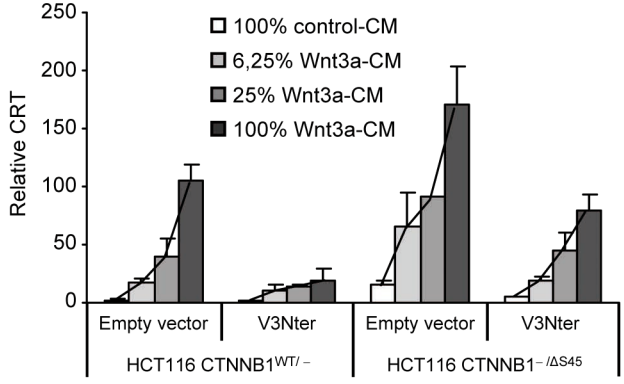

c

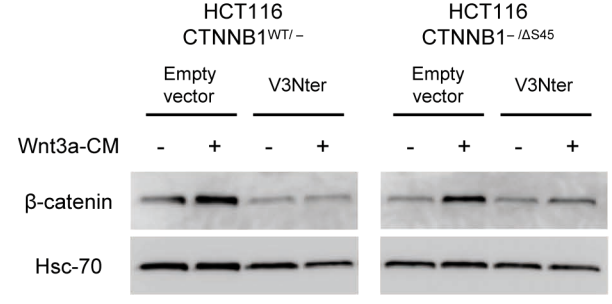

d

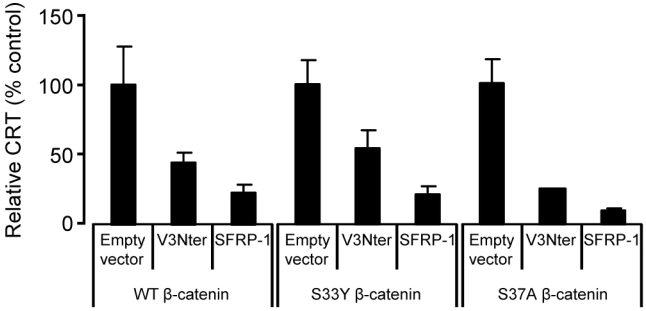

Figure 4 - Lavergne *et al.*

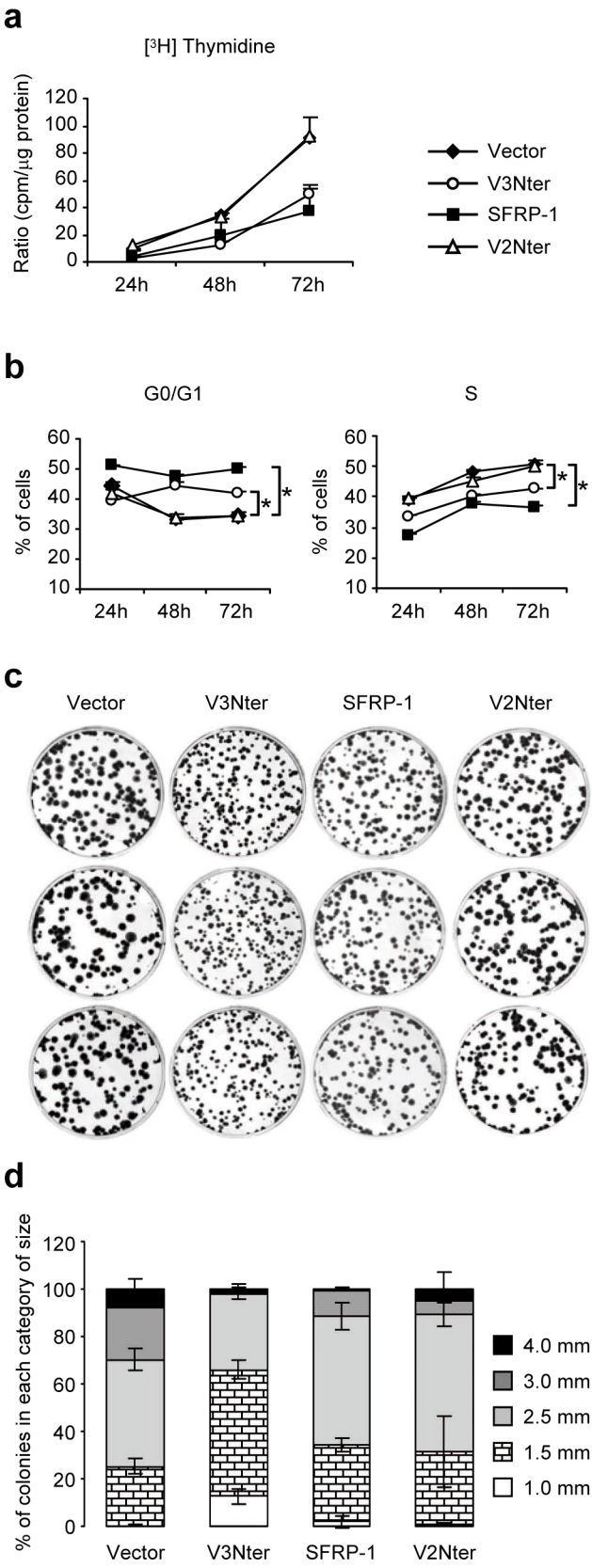

Figure 5 - Lavergne *et al.*

a

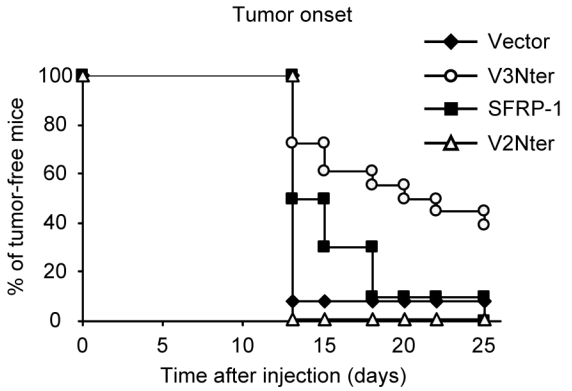

b

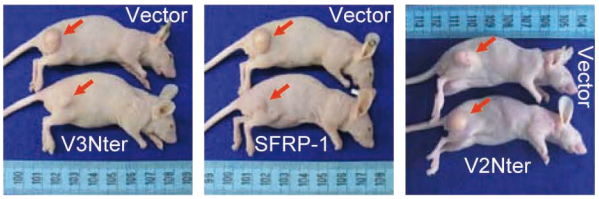

c

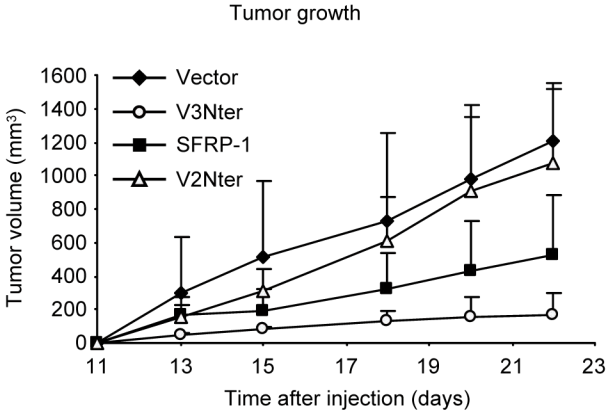

d

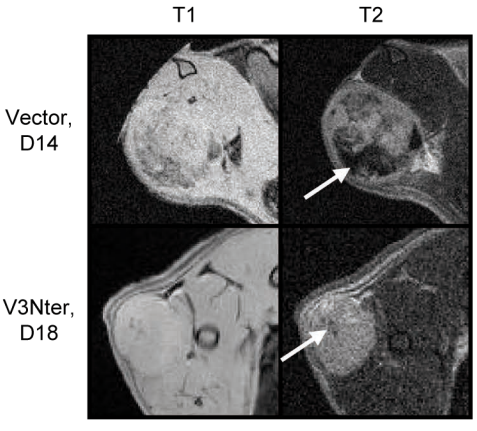

Figure 6 - Lavergne *et al.*

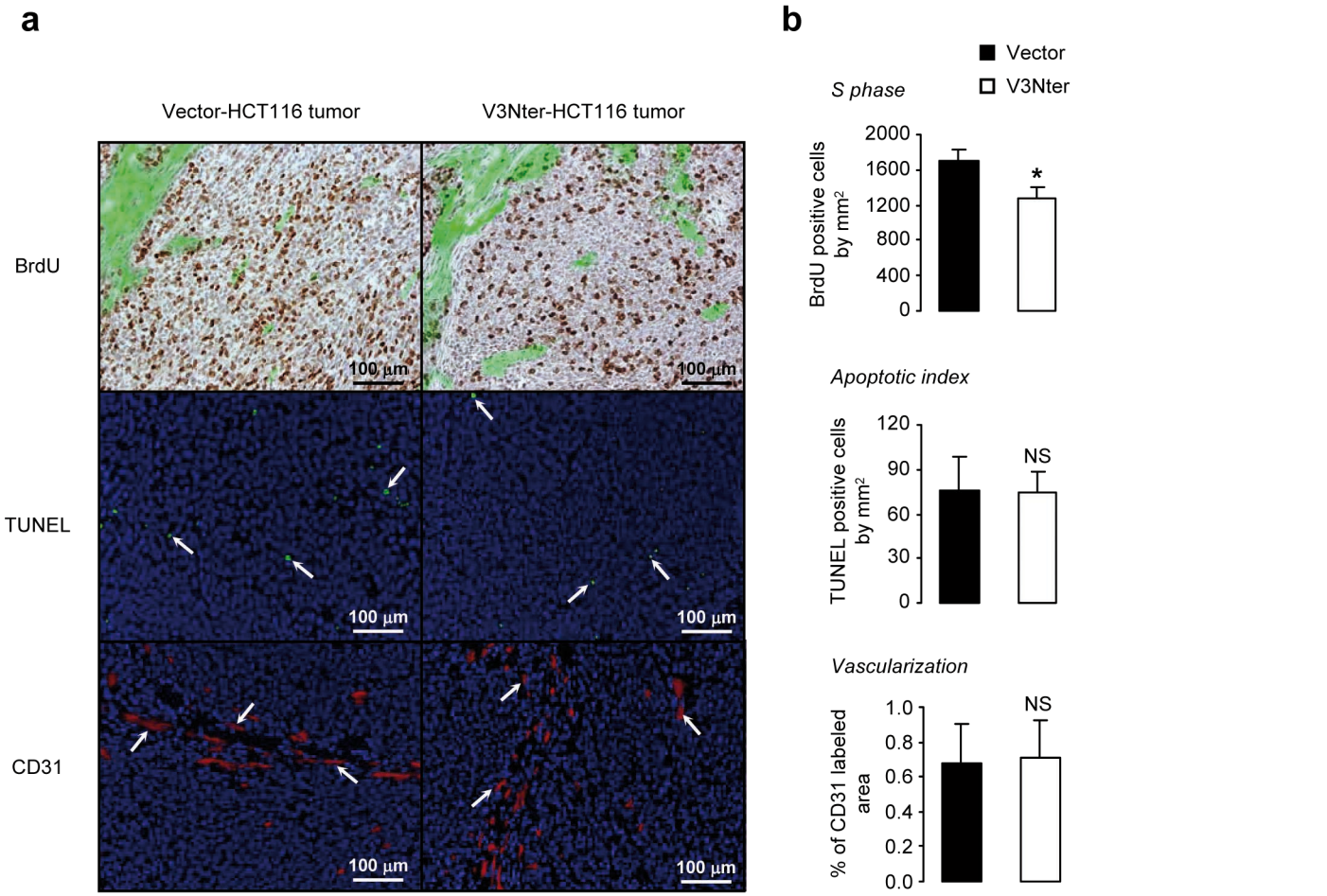

Figure 7 - Lavergne *et al.*

a

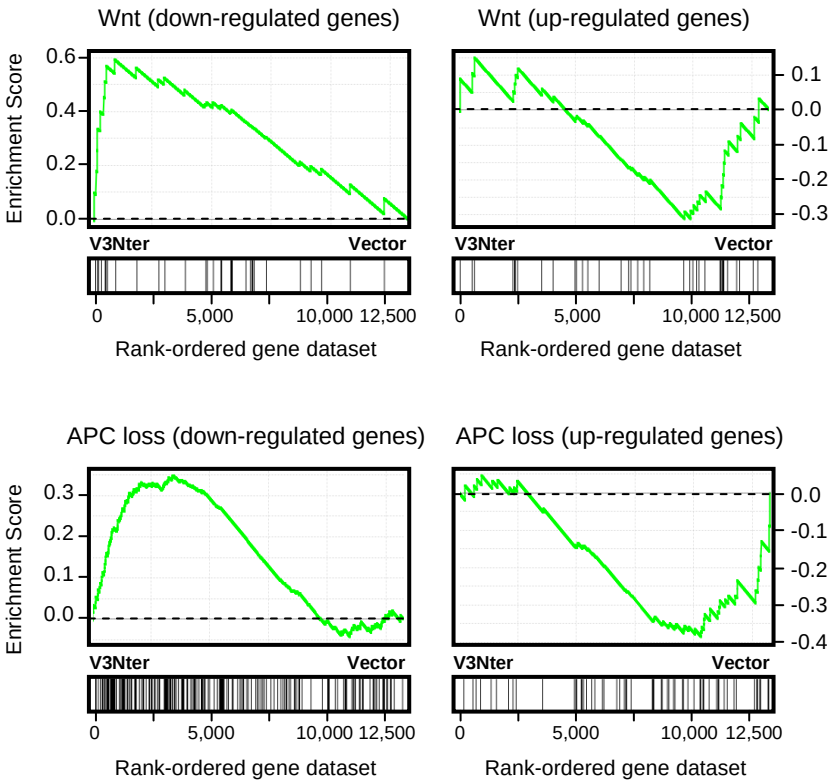

b